Rupture process of the 2005 West Off Fukuoka Prefecture, Japan, earthquake

Haruo Horikawa

Active Fault Research Center, National Institute of Advanced Industrial Science and Technology (AIST), Tsukuba, Ibaraki 305-8567 Japan

The 2005 West off Fukuoka Prefecture, Japan, earthquake (M_S 6.7) is a moderate-size crustal event. The rupture process of this earthquake was inferred from strong motion data. It is observed regardless of epicentral distance and azimuth that the initial P-wave with a small amplitude continued for 2.5–4 s, suggesting prominent initial rupture. The duration of the initial rupture was estimated to be 3.3 s from travel time analysis. Inversion analysis shows that the initial rupture continued for 3.5 s and the overall rupture finished within 10 s. An area of large slip with two peaks of slip amount appeared to the southeast of the hypocenter, and the location of the large-slip area is consistent with the origin of the main rupture inferred from travel time analysis. Small amount of slip was found at and around the hypocenter, and the rupture velocity was slow there. The seismic moment of this earthquake was estimated to be 5.7×10^{18} Nm (M_w 6.4). The maximum stress drop calculated from the derived slip distribution exceeded 10 MPa. An area of negative stress drop expanded, corresponding to the distribution of small slip. Forward modeling of the observed waveforms suggests that the negative stress drop is not fully attributable to poor resolution of inversion analysis for small amount of slip. Since dynamic stress drop should be positive around the hypocenter so that rupture propagates over the entire fault, it is plausible that the negative stress drop appeared after healing.

Key words: 2005 Fukuoka earthquake, strong motion data, nucleation phase, dynamic stress drop, negative stress drop.

1. Introduction

The 2005 West Off Fukuoka Prefecture, Japan, earthquake (M_S 6.7) is a moderate-size crustal event, and unexpectedly occurred in southwest Japan. The source region of this earthquake previously experienced low earthquake activity (Fig. 1(a)). Active faults systems responsible for the 2005 Fukuoka earthquake is not known, and no historical earthquakes that are believed to be previous events of this earthquake are known either. Focal mechanism determined from P-wave first motions and a moment tensor solution are consistent with each other in that strike slip occurred on a NW–SE striking vertical plane or NE–SW striking vertical plane (Ito *et al*., 2006). Aftershocks extended bilaterally to NW and SE from the hypocenter for a distance of about 25 km, suggesting that rupture propagated bilaterally on a NW–SE striking fault (Fig. 1(b)).

The lack of seismic data before the 2005 Fukuoka earthquake means that the 2005 Fukuoka earthquake provides a valuable opportunity for investigating characteristics of strong motions in the Fukuoka area that is one of the most populated areas in Japan. This investigation may be urgent when considering the effect of stress change caused by the 2005 Fukuoka earthquake. It is suggested that the Kego fault system, which is located in the southern part of the Fukuoka area (Fig. 1), has become closer to failure owing to the stress change (e.g. Toda and Horikawa, 2005). An-

other fault systems will also experience stress change, and the stress change will affect the earthquake occurrence on these fault systems. It is necessary to evaluate the effect for seismic hazard assessment. In order to facilitate these studies, a fault model of the 2005 Fukuoka earthquake is needed.

In this study, a fault model of the 2005 Fukuoka earthquake is constructed, and the overall rupture process of the 2005 Fukuoka earthquake is inferred from strong motion records. A notable character of the 2005 Fukuoka earthquake is that the ground motions with a small amplitude continued for an unusually long time from the beginning. I analyzed travel time to grasp the character of this initial phase. I then invert strong motion data for slip and rupture time distributions. Finally I calculated static change of shear traction (stress drop), finding that an area of negative stress drop exists near the hypocenter.

2. Travel Time Analysis

An example of the initial part of the P-wave is displayed in Fig. 3(a). This low amplitude P-wave can be seen regardless of epicentral distance or azimuth. Hence it is plausible that the small amplitude is related to the source process. Moreover, the duration systematically changes (Fig. 3(b)). The duration is the shortest to the southeast of the hypocenter, and it becomes longer as the azimuth is away from the direction. This suggests that the initial part of the rupture emitted small seismic waves, and the starting point of the main rupture is located to the southeast of the hypocenter.

Both hypocenter and the origin of the main rupture phase were determined in order to clarify the duration of the initial
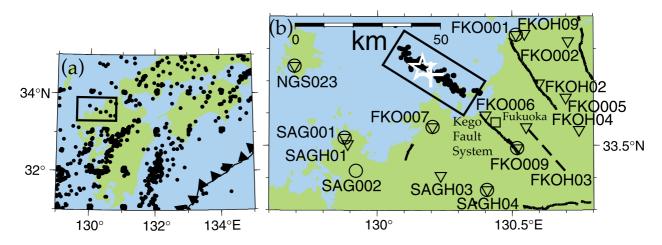
Fig. 1. (a) Seismicity of southwestern Japan from January 1990 to March 20, 2005 (just before the 2005 West Off Fukuoka Prefecture earthquake) in which events with M ≥ 3 and with depth ≤ 30 km are plotted from the earthquake catalogue of the Japan Meteorological Agency. The rectangle area corresponds to the region displayed in panel (b). (b) Map of the source region of the 2005 Fukuoka earthquake. Aftershocks with M ≥ 3 that occurred by the end of July are plotted with black dots. The locations of the aftershocks were redetermined in this study. The epicenters of the initial rupture and main rupture are displayed with star and cross, respectively. Bold lines stand for active faults (Nakata and Imaizumi, 2002). The inverted triangles show the stations used in travel time analysis, and circles stand for those used in inversion analysis. The inclined rectangle corresponds to the region shown in Fig. 2.
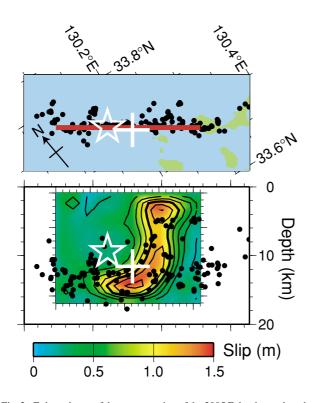

Fig. 2. Enlarged map of the source region of the 2005 Fukuoka earthquake. Aftershocks are plotted with black dots. The criterions for choosing the aftershocks are the same as those of Fig. 1. The red line stand for the upper edge of the assumed fault plane used in the waveform analysis. A cross section along the assumed fault strike (N122°E) is also shown with the slip distribution inferred in this study.
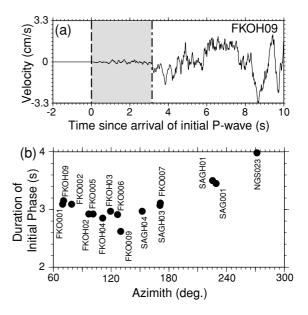

Fig. 3. (a) An example of long initial phase observed during the 2005 West Off Fukuoka Prefecture earthquake. The original vertical-component accelerogram was high-pass filtered above 0.1 Hz and integrated into velocity. The Dashed line stands for the arrival of initial *P*-wave, and the dash-dotted line means the arrival of "main" *P*-wave. The shaded area is thus identified as initial phase in this study. (b) Azimuthal dependence of the duration of initial phase.

rupture stage and the relative location of the main rupture to the initial rupture. Only arrival times of *P*-wave were manually picked for 15 stations shown with inverse triangles in Fig. 1(b), and were used in this analysis. It is desirable to use arrival times of *S*-wave for more precise determination of the locations (e.g. Gomberg *et al*., 1990), but, in this case, it is quite difficult to pick the arrival of *S*-wave at each sta-

tion, particularly arrival times of *S*-wave corresponding to the initial rupture. The velocity structure was assumed to be horizontally stratified as given in Table 1. This velocity structure was used by Nakamichi and Kawase (2002).

The epicenter and the horizontal location of the origin of the main rupture are shown in Figs. 1(b) and 2. The origin of the main rupture is located 3.6 km to the southeast of the epicenter. The depths of the hypocenter of the initial rupture and the main rupture were 9 km and 13 km, respectively. Hence the distance of the two "hypocenters"

Table 1. Velocity structure assumed in this study.

D_{upper}	V_P	V_S	ρ	Q_P	Q_S
0.0	3.2	2.0	2.1	200	100
0.1	5.15	2.85	2.5	300	150
3.0	5.5	3.2	2.6	400	200
6.0	6.0	3.46	2.7	600	300
19.0	6.7	3.87	2.8	800	400
34.0	7.8	4.5	3.2	1000	500

D_{upper}: Upper depth of a layer (km), V_P: P-wave velocity (km/s), V_S: S-wave velocity (km/s), ρ: Density (g/cm^3).

was 5.0 km. The estimated origin time of the main rupture is later by 3.3 s than that of the initial rupture. The average rupture velocity of the initial rupture stage is estimated to be 1.5 km/s. This rupture velocity agrees well with the average value of the rupture velocity at the nucleation stage estimated by Beroza and Ellsworth (1996)

Similar analyses are presented in this volume (Sekiguchi *et al.*, 2006; Takenaka *et al.*, 2006). All results has a common character in that the origin of the main rupture is located to the southeast of hypocenter. However, the relative depth of the origin of the main rupture to the hypocenter is different. The origin of the main rupture is shallower than the hypocenter in Takenaka *et al.* (2006). On the other hand, the origin of the main rupture is deeper than the hypocenter in this study and Sekiguchi *et al.* (2006). These authors have used different data sets (i.e., different combination of stations) and velocity structure. The difference will affect the results.

3. Inversion Analysis

Three-component strong motion records of 12 stations shown with circles in Fig. 1(b) were used in this analysis. The vertical component of SAG002, however, was excluded because of a mechanical problem. The original accelerograms were band-pass filtered between 0.1 and 1 Hz, and numerically integrated twice into displacement. The data length was set to be 30 s from the onset of P-wave for all stations.

The inversion method for analyzing the rupture process was the same as that of Horikawa (2001). An assumed fault plane was divided into small segments called subfaults, and both slip and rupture starting time of each subfault were inferred from observed ground motions with a recursive inversion procedure proposed by Matsu'ura and Hasegawa (1987). Derived solutions strongly depend on the starting models of the recursive procedure. Thus we have to solve the equation system from different starting models in order to reduce the effect of the dependence. The detail of the starting models used in this study will be described later.

The ground-motion contribution from each subfault was expressed with the response of a point source located at the center of the subfault. The point-source response or Green's function was calculated with the reflectivity method by Takeo (1985). A horizontally stratified anelastic medium given in Table 1 was assumed in the calculation.
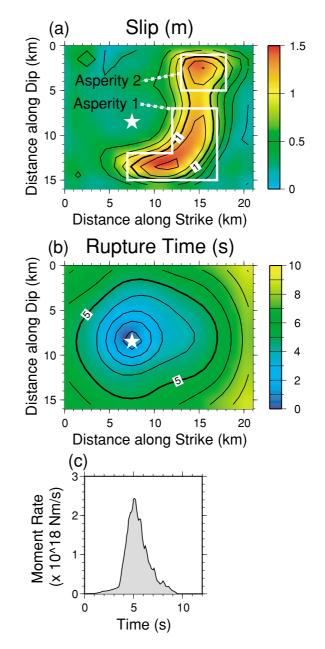

Fig. 4. Fault model of the 2005 West Off Fukuoka Prefecture earthquake derived from inversion of strong motion data. (a) Slip distribution. The contour lines start at 0.2 m, and continue with 0.2 m intervals. (b) Rupture time distribution. The contour lines start at 1 s, and continue with 1 s intervals. The stars in the upper two panels stand for the hypocenter. (c) Seismic moment rate function.

4. Result of Inversion Analysis

The 2005 Fukuoka earthquake was modeled with a single planar fault that had 21 km length and 16 km width. The upper edge of the fault plane is located at a depth of about 0.9 km. The focal mechanism was fixed to 122° of strike, 89° of dip angle, and 8° of rake angle. These values were adopted from the Harvard quick CMT solution.

Different rupture velocities were assigned on the initial rupture and the "main" rupture when assuming starting models used in the recursive inversion procedure. Seven values were assumed for the time when the rupture velocity changed. Combination of these assumptions yields tens of starting models, and inversion analysis was done for all
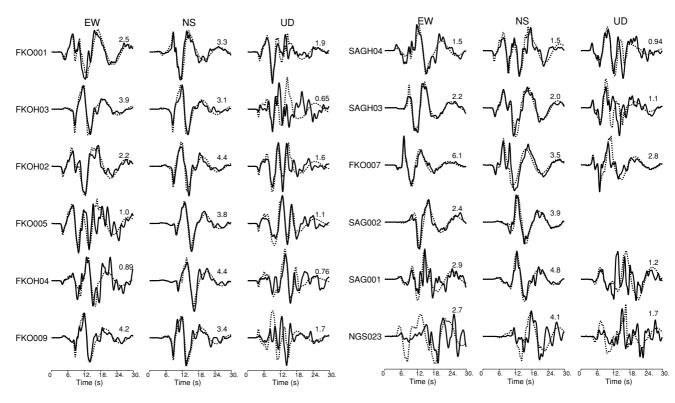
Fig. 5. Comparison of observed (solid) and synthetic (dashed) waveforms. The origin of time axis is the arrival of *P*-wave. The numeral attached to the end of each trace stands for peak amplitude of the observed waveforms in centimeter.

of these starting models. I adopted the inversion result that yielded the least residual.

The derived slip distribution is displayed in Fig. 4(a). The average slip is 0.54 m, and the maximum slip almost reaches 1.5 m. As suggested by the observed waveforms (Fig. 3), slip around the hypocenter is small and less than 0.4 m. A region of large slip (> 1 m) was revealed to the southeast of the hypocenter, extending from a shallow part of the fault plane to the bottom. The relative location of the region of large slip (so-called asperity) agrees with the result of travel time analysis that the breakage of the main rupture occurred to the southeast of the hypocenter. Two peaks of slip are seen within the area of large slip, and the two peaks have the almost same maximum value of slip. The seismic moment was estimated to be 5.7×10^{18} Nm (M_w 6.4).

Figure 4(b) shows the distribution of rupture starting time over the fault. The rupture slowly spread during the first 3 s. Then, the rupture spreading to the southeastern part of the fault abruptly accelerated in the middle depth of the fault. Rupture propagation was also accelerated when it passed over a deeper part of the asperity at a time between 4 and 5 s. After five seconds (5 s) from the starting of the rupture, rupture propagation decelerated, and finished striking the edges of the assumed fault.

The rupture progress to the northwestern part of the fault abruptly changed at 3 s after the beginning of the rupture. However, it should be noted that this character is almost the same as that of the initial model used in the inversion. I suspect that the rupture propagation to the northwestern part of the fault is poorly resolved because few stations are located at this azimuth and slip amount is generally small in

the northeastern part of the fault.

Figure 4(c) shows the seismic moment rate function. The overall feature of the moment rate function was quite simple, and the main part was well-approximated with a triangle of the duration of about 4 s. The rupture finished within 10 s. As suggested by slip and rupture time distributions, the moment release was small during the first 3.5 s, and then the moment release abruptly increased. The duration of the small moment release in the beginning of rupture shows good agreement with the time difference between initial rupture and main rupture inferred from the travel time analysis.

The nucleation stage of the 2005 Fukuoka earthquake is "unbalanced" with the eventual size of the earthquake. According to the empirical relationships between the duration of nucleation phase and eventual seismic moment (Beroza and Ellsworth, 1996; Umeda *et al.*, 1996), the eventual seismic moment derived in this study predicts that the nucleation phase will continue for about 1 s, which is much shorter than the observed value for this earthquake. The seismic moment released during the nucleation phase (first 3.5 s) was estimated to be 2.1×10^{17} Nm, and the ratio of this seismic moment to the eventual seismic moment was 4%. This ratio is much larger than the average value (0.4%) estimated by Beroza and Ellsworth (1996).

Figure 5 shows comparison of the observed and synthetic waveforms. Generally, the horizontal components show good fit to the observed strong motions, and the vertical components matches worse to the observed ones.

Figure 6 shows how the two asperities defined in Fig. 4 contribute to the synthetic waveforms. The relative contribution of the two asperities depends on azimuth from the
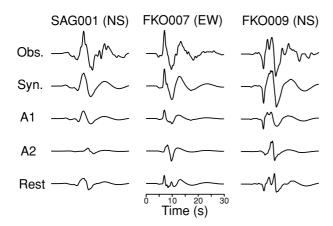
Fig. 6. Comparison of data (top trace) and synthetics (second trace) with contributions to the synthetics from Asperity 1 (third trace) and Asperity 2 (fourth trace) and the rest of the fault plane (bottom trace). The region of asperities are defined in Fig. 4.
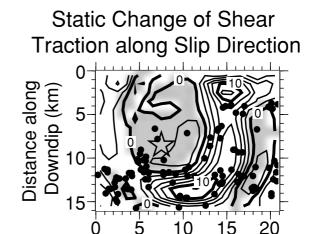

Fig. 7. Distribution of static change of shear traction along slip direction (stress drop). The contour interval is 2 MPa, and the gray regions consist of subfaults of negative stress drop. The star stands for the hypocenter. Aftershocks with $M \geq 3$ are also plotted with closed circles.

fault plane. The shallower asperity (Asperity 2) contributes to the synthetics less significantly than the deeper one (Asperity 1) when a station is located nearly normal to the fault plane (SAG001). On the other hand, the contribution of the Asperity 2 is comparable to that of the Asperity 1 (FKO007) and even larger than that of the Asperity 1 (FKO009) when azimuth of a station is close to the fault strike.

This variation is attributable to the effect of the rupture directivity. Although both asperities are located to the same direction for fault strike, their locations are different for fault dip. The direction of the rupture propagation from the hypocenter to and across the Asperity 2 coincides with that of the near-source stations located close to the fault strike. Hence the rupture directivity works effectively for such stations. On the other hand, the contribution of the Asperity 2 is comparable to that of the Asperity 1 (FKO007) when azimuth of a station is close to the fault strike. The amplitude of the contribution of the Asperity 2 is even larger than that of the Asperity 1 (FKO009).

Figure 7 shows the distribution of static change of shear traction (static stress drop). The calculation was done with analytical expression of static deformation by Okada (1992) (Kubota *et al.*, 1997). An area of large slip corresponds to that of large stress drop. The maximum value of stress drop exceeds 10 MPa, which is observed in other Japanese intraplate earthquakes (e.g. Miyatake, 1992). Small slip at and around the hypocenter corresponds to negative stress drop that vastly expanded there.

The hypocenters of aftershocks are plotted with the slip distribution (Fig. 2) and the distribution of static stress drop (Fig. 7). The aftershocks are distributed nearby the peak of slip especially the Asperity 1, and do not preferentially distribute in areas of negative stress drop.

Finally, I will briefly compare my slip model with other models presented in this issue (Asano and Iwata, 2006; Sekiguchi *et al.*, 2006). The Sekiguchi's model has only one asperity at a shallow part of a fault, and the Asano's model and my model have two asperities whose locations are similar between the two models. However, the Asano's shallow asperity is larger than deeper one in size while

my shallow asperity is smaller than deeper one. Hence Sekiguchi's model and my model are end members, and Asano's model is between the two.

5. Concluding Remarks

A notable character of this earthquake is that initial phase with a small amplitude continued for unusually long time of 3.5 s. This prominent initial phase corresponds to the wide area of negative static stress drop at and around the hypocenter shown in Fig. 7. If this negative stress drop appears during slippage of the corresponding region, this means velocity strengthening, and the corresponding area is a sink of energy (e.g., Scholz, 2002). If such energy sink appears around the hypocenter, rupture will not propagate over the entire fault. Hence it is plausible that the negative static stress drop appeared after healing. If this is the case, the healing there was so strong that the slip did not occur again after the healing although stress was rebuilt up owing to rupture of the adjacent region. The rebuilt stress was kept during the rupture of the mainshock, and resulted in negative stress drop.

However, we have to examine carefully the validity of the negative stress drop before considering implications of the negative stress drop. This is because inversion analysis has poor resolution for small amount of slip. The residual between the observed waveforms and the synthetics will substantially reduce when a derived fault model can explain parts of waveforms with a large amplitude. I checked the sensitivity of the observed waveforms to slip amount around the hypocenter. I calculated waveforms resulting from a fault model that had an additional slip of 0.4 m to the region around the hypocenter. The resultant slip amount near the hypocenter exceeded the average slip calculated before the addition, and diminished most of the negative stress drop around the hypocenter. Although some of the synthetic waveforms resulting from the modified slip distribution showed slightly better fit to the observed ones, other synthetic waveforms showed substantially worse fit to the

observed ones, and the resultant residual becomes worse after the modification. Hence I believe that the negative stress drop is not fully attributable to the poor resolution of inversion analysis. The initial part of P-waves should be carefully analyzed in order to investigate more rigorously the time history of stress at and around the hypocenter of the 2005 Fukuoka earthquake.

References

Aoi, S., K. Obara, S. Hori, K. Kasahara, and Y. Okada, New strong-motion observation network: KiK-net, *EOS, Trans. AGU*, **81**, F863, 2000.

Asano, K. and T. Iwata, Source process and near-source ground motions of the 2005 West Off Fukuoka Prefecture earthquake, *Earth Planets Space*, **58**, this issue, 93–98, 2006.

Beroza, G. C. and W. L. Ellsworth, Properties of the seismic nucleation phase, *Tectonophysics*, **261**, 209–227, 1996.

Gomberg, J. S., K. M. Shedlock, and S. W. Roecker, The effects of S-wave arrival times on the accuracy of hypocenter estimation, *Bull. Seism. Soc. Am.*, **80**, 1605–1628, 1990.

Horikawa, H., Earthquake doublet in Kagoshima, Japan: Rupture of asperities in a stress shadow, *Bull. Seism. Soc. Am.*, **91**, 112–127, 2001.

Ito, Y., K. Obara, T. Takeda, K. Shiomi, T. Matsumoto, S. Sekiguchi, and S. Hori, Initial rupture fault, main-shock fault, and aftershock faults: Fault geometry and bends inferred from centroid moment tensor inversion of the 2005 west off Fukuoka prefecture earthquake, *Earth Planets Space*, **58**, this issue, 69–74, 2006.

Kinoshita, S., Kyoshin net (K-NET), *Seismol. Res. Lett.*, **69**, 309–332, 1998.

Kubota, Y., M. Yamamoto, T. Miyatake, and T. Mikumo, Static stress drop distribution of large earthquakes, *Programme and Abstracts of Japan Earth and Planetary Science Joint Meeting*, **1**, 791, 1997.

Matsu'ura, M. and Y. Hasegawa, A maximum likelihood approach to nonlinear inversion under constraints, *Phys. Earth Planet. Int.*, **47**, 179–187, 1987.

Miyatake, T., Dynamic rupture processes of inland earthquakes in Japan: weak and strong asperities, *Geophys. Res. Lett.*, **19**, 1041–1044, 1992.

Nakamichi, S. and H. Kawase, Broadband strong motion simulation in Fukuoka City based on a three-dimensional basin structure and a hybrid method, *Journal of Structural and Construction Engineering, AIJ*, **560**, 83–91, 2002.

Nakata, T. and T. Imaizumi, *Digital Active Fault Map of Japan*, University of Tokyo Press, Tokyo, 2002.

Okada, Y., Internal deformation due to shear and tensile faults in a halfspace, *Bull. Seism. Soc. Am.*, **82**, 1018–1040, 1992.

Scholz, C. H., *Mechanics of Earthquakes and Faulting, 2nd edition*, 471 pp, Cambridge University Press, Cambridge, 2002.

Sekiguchi, H., S. Aoi, R. Honda, N. Morikawa, T. Kunugi, and H. Fujiwara, Rupture process of the 2005 West Off Fukuoka Prefecture earthquake obtained from strong motion data of K-NET and KiK-net, *Earth Planets Space*, **58**, this issue, 37–43, 2006.

Takenaka, H., T. Nakamura, Y. Yamamoto, G. Toyokuni, and H. Kawase, Precise location of the fault plane and the onset of the main rupture of the 2005 West Off Fukuoka Prefecture earthquake, *Earth Planets Space*, **58**, this issue, 75–80, 2006.

Takeo, M., Near-field synthetic seismograms taking into account of the effects of anelasticity—The effects of anelastic attenuation on seismograms caused by a sedimentary layer, *Meteorol. Geophys.*, **36**, 245–257, 1985 (in Japanese with English abstract).

Toda, S. and H. Horikawa, Stress transferred by the M 7.0 Fukuoka-kenseiho-oki earthquake: Influence on the Kego Fault beneath the city of Fukuoka, *Abstracts of the 2005 Japan Earth and Planetary Science Joint Meeting*, x113p-025, 2005.

Umeda, Y., T. Yamashita, T. Tada, and N. Kame, Possible mechanisms of dynamic nucleation and arresting of shallow earthquake faulting, *Tectonophysics*, **261**, 179–192, 1996.

Wessel, P. and W. H. F. Smith, New, improved version of Generic Mapping Tools released, *Eos*, **79**, 579, 1998.

H. Horikawa (E-mail: h.horikawa@aist.go.jp)